

1175. Stability and local bifurcation analysis for a nonlinear coupled helicopter blade-absorber system via normal form method

Wei Zhou¹, Jinglong Han²

State Key Laboratory of Mechanics and Control of Mechanical Structures
Nanjing University of Aeronautics and Astronautics, Nanjing, 210016, China

¹Corresponding author

E-mail: ¹rose_99405@163.com, ²hjlac@nuaa.edu.cn

(Received 31 October 2013; received in revised form 5 December 2013; accepted 12 December 2013)

Abstract. Consider the effect of nonlinear spring and linear viscous damping in structure, the motion equations of a helicopter blade-absorber system has been established by Lagrange equation. Since the helicopter blade-absorber system exists motion coupling, the inertia and stiffness terms of equations are decoupled via equivalent principal coordinate transformation. The stability and local bifurcation behaviors of the principal coordinate equations are investigated with the aid of multiple scales method and normal form theory. Two kinds of critical points for the bifurcation response equations near the combination resonance are considered, which are characterized by a pair of purely imaginary eigenvalues and double zero eigenvalues. The Hopf bifurcation solution, bifurcation path, and transition curves of the model are investigated respectively. For each case, the numerical results obtained by Runge-Kutta method coincide with the analytical predictions. These results may provide some guidance for parameter design of helicopter blade-absorber system.

Keywords: nonlinear coupled blade-absorber model, local bifurcation, stability, normal form.

1. Introduction

Normal form method is one of the basic methods in the study of nonlinear vibration. The essential idea of the normal form method is using successive coordinate transformations to systematically establish the simplest possible form of the original differential equations. The simple form can demonstrate all possible dynamical properties of the original system in the neighborhood of the bifurcation point. Normal forms are generally not uniquely defined, and finding a normal form for a given system of differential equations is not a simple task. In recent years, normal form methods have got much development. Among them, Yu et al. have proposed and improved a normal form method with a combination of perturbation analysis and computer algebra in [1-8]. Since the reduced system obtained by this normal form method can be more convenient to study bifurcation and stability, Zhang [9] studied the local bifurcation of a nonlinear viscoelastic panel in supersonic flow model via this method, which is characterized by a pair of purely imaginary eigenvalues. Subsequently, she and coauthors researched the stability and local bifurcation of functionally graded material plate under transversal and in-plane excitations in [10]. In addition, Zhou et al. studied several dynamical behaviors for a two degrees of freedom pitch-roll ship via this normal form method in [11]. Wang et al. [12] research on the stability and bifurcation for a flexible beam under a large linear motion with a combination parametric resonance.

Vibration problem has always restricted the development of helicopter, and it is also an important problem which scholars have been dedicated to research and solve. During flight, there are many factors leading to helicopter vibration. In particular, blade flapping, lagging and aerodynamical action can make a significant rotor vibration, meanwhile, fuselage vibration transfers along hub and interacts with rotor, which will aggravate overall vibration. In order to reduce the vibration level of helicopter blade and fuselage, people take a method of setting absorber on blade or hub. For instance, absorbers installed on Boeing Vertol 347, Lynx and Black Hawk have been achieved satisfactory effects [13, 14]. However, if absorber parameters are designed unreasonable, not only may generate resonance phenomenon, but also may cause entire

system instability or even leading to a disastrous consequences [15, 16]. Therefore, the research on helicopter blade-absorber system dynamics behavior is of important theoretical and practical significance.

Helicopter blade-absorber system not only contains complex nonlinear structure but also exists motion coupling between each degrees of freedom, therefore, its mathematical modeling and theoretical analysis both have certain difficulties. At present, the research on this system usually adopts experiment or numerical simulation [17-20]. Since the analysis objects of analytic method generally can not be too complicated, the qualitative study on helicopter blade-absorber system is relatively rare [13, 21, 22]. Among them, Nagasaka et al. [21, 22] respectively established two degrees of freedom blade-absorber and three degrees of freedom blade-absorber-fuselage model, numerical simulated the vibration response and verified the numerical results by van der Pol method. However, in the above two models, only linear structure is considered, and it is obviously not enough for the in-depth study on dynamical behaviors.

In view of the above problems, in this paper the normal form method proposed by Yu will be first introduced to the dynamics analysis of helicopter blade-absorber system, also, at modeling time, structure nonlinear will be considered. Firstly, establish a helicopter blade-absorber model by Lagrange equation. As the helicopter blade-absorber system exists motion coupling, the inertia and stiffness terms of equations are decoupled via equivalent principal coordinate transformation. The stability and local bifurcation behaviors of the principal coordinate equations are investigated with the aid of multiple scales method and normal form theory. Two kinds of degenerated equilibrium points of the bifurcation response equations are considered, which are characterized by a pair of purely imaginary eigenvalues and a pair of complex conjugate having negative real part as well as a double zero eigenvalues. Finally, Hopf bifurcation solution, bifurcation path and transition curves are obtained. The analytical predictions agree with the results of Runge-Kutta method.

This paper is organized as follows: in Section 2, a helicopter blade-absorber model is established. In Section 3, the bifurcation response equations near combination resonance are obtained using multiple scales method. The detailed stability and local bifurcation analysis of the bifurcation response equations in the vicinity of the critical points are given in Section 4, which is followed in Section 5 by a short conclusion.

2. Helicopter blade-absorber modeling

This paper focuses on the stability and local bifurcation behaviors of a helicopter blade-absorber system. Consider pendulum absorber is designed in helicopter blade flapping direction, and there is a harmonic excitation $y_0 R \cos \omega_0 t$ acting on rotor hub position. The connections of blade-hub and blade-absorber are simplified as damping and elastic hinge restrictions. The horizontal displacement of hub is omitted. The blade-absorber system physical model is shown in Fig. 1. Aerodynamic force model adopts blade micro segment aerodynamic force $\Omega^2 F_b \cos \omega_1 t$, which can be found in [22].

Take blade flapping angle β_1 and absorber swinging angle (relative to the blade) β_2 as generalized coordinate. Let upward direction is positive. The coordinate of blade micro segment $mRdr$ on the rR position is:

$$\begin{aligned} x_1 &= (e + r \cos \beta_1) R, \\ z_1 &= (r \sin \beta_1 + y_0 \cos \omega_0 t) R. \end{aligned} \tag{1}$$

If blade rotates with angular velocity Ω , then its velocity in Y direction is:

$$\dot{y}_1 = x \Omega. \tag{3}$$

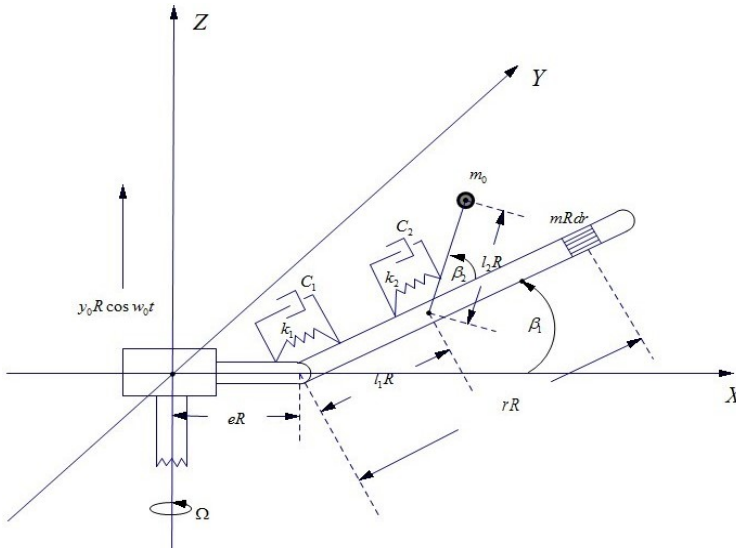


Fig. 1. Physical model of a helicopter blade-absorber system

The coordinate of absorber mass m_0 is:

$$x_2 = [e + l_1 \cos \beta_1 + l_2 \cos(\beta_1 + \beta_2)]R, \quad (4)$$

$$z_2 = [l_1 \sin \beta_1 + l_2 \sin(\beta_1 + \beta_2) + y_0 \cos \omega_0 t]R. \quad (5)$$

It has Y direction velocity:

$$\dot{y}_2 = x\Omega. \quad (6)$$

Using Lagrange equation and small angle assumption, blade-absorber system flapping motion equations can be obtained as follows:

$$\begin{aligned} R^2 \left[\frac{1}{3} (1 - e)^3 mR + (l_1 + l_2)^2 m_0 \right] \ddot{\beta}_1 + R^2 l_2 m_0 (l_1 + l_2) \ddot{\beta}_2 \\ + \Omega^2 R^2 \left\{ \left[\frac{1}{2} (1 - e)^2 e + \frac{1}{3} (1 - e)^3 \right] mR + [(l_1 + l_2)^2 + e(l_1 + l_2)] m_0 \right\} \beta_1 \\ + \Omega^2 R^2 l_2 m_0 (e + l_1 + l_2) \beta_2 + k_1(\beta_1) + c_1(\dot{\beta}_1) \end{aligned} \quad (7)$$

$$\begin{aligned} = R^2 \omega_0^2 y_0 \cos(\omega_0 t) \cdot \left[\frac{1}{2} (1 - e)^2 mR + (l_1 + l_2) m_0 \right] + R^2 \Omega^2 F_b \cos(\omega_1 t) (1 - e), \\ R^2 l_2 m_0 (l_1 + l_2) \ddot{\beta}_1 + R^2 l_2^2 m_0 \ddot{\beta}_2 + \Omega^2 R^2 l_2 m_0 (e + l_1 + l_2) \beta_1 \\ + \Omega^2 R^2 l_2 m_0 (e + l_1 + l_2) \beta_2 + k_2(\beta_2) + c_2(\dot{\beta}_2) = l_2 m_0 R^2 \omega_0^2 y_0 \cos(\omega_0 t), \end{aligned} \quad (8)$$

where $k_1(\beta_1)$, $k_2(\beta_2)$, $c_1(\dot{\beta}_1)$, $c_2(\dot{\beta}_2)$ are blade-absorber hinge-spring and hinge-damping constitutive relation respectively. For linear viscous damper and weak nonlinear spring condition, there are:

$$c_1(\dot{\beta}_1) = \varepsilon c'_1 \dot{\beta}_1, \quad c_2(\dot{\beta}_2) = \varepsilon c'_2 \dot{\beta}_2, \quad (9)$$

$$k_1(\beta_1) = k_1 \beta_1 + \varepsilon k_2 \beta_1^2 + \varepsilon k_3 \beta_1^3, \quad k_2(\beta_2) = k_4 \beta_2 + \varepsilon k_5 \beta_2^2 + \varepsilon k_6 \beta_2^3, \quad (10)$$

where ε is a small parameter and $\varepsilon > 0$.

Supposing $\omega_0 = \omega_1 = \Omega$, $\psi = \Omega t$, and applying dimensionless method, Eq. (7) and (8) can be simplified as follows:

$$\beta_1'' + a_1\beta_1' + \omega_1^2\beta_1 + b_1\beta_2 + \varepsilon(c_1\beta_1' + d_1\beta_1^2 + e_1\beta_1^3) = f_1\cos(\omega\psi), \tag{11}$$

$$\beta_2'' + a_2\beta_2' + b_2\beta_1 + \omega_2^2\beta_2 + \varepsilon(c_2\beta_2' + d_2\beta_2^2 + e_2\beta_2^3) = f_2\cos(\omega\psi), \tag{12}$$

where $a_1 = l_2(l_1 + l_2)\gamma\Delta$, $b_1 = l_2\gamma(e + l_1 + l_2)\Delta$, $c_1 = 2\eta_1\omega\beta_1/[1 + 3(l_1 + l_2)^2\gamma/(1 - e)^3]$,

$$d_1 = \frac{k_2\gamma}{\Omega^2 R^3 m}, e_1 = \frac{k_3\Delta}{\Omega^2 R^3 m}, f_1 = \left\{ \left[\frac{1}{2}(1 - e)^2 + (l_1 + l_2)\gamma \right] y_0 + F_b(1 - e) \right\} \omega^2 \Delta,$$

$$\omega_1 = \sqrt{\left\{ \frac{1}{2}(1 - e)^2 e + \frac{1}{3}(1 - e)^3 + [(l_1 + l_2)^2 + e(l_1 + l_2)]\sigma \right\} \cdot \gamma + \frac{\omega_{\beta_1}^2}{[1 + 3(l_1 + l_2)^2\gamma/(1 - e)^3]}}$$

$$a_2 = 1 + \frac{l_1}{l_2}, b_2 = 1 + \frac{e}{l_2} + \frac{l_1}{l_2}, \omega_2 = \sqrt{1 + \frac{e}{l_2} + \frac{l_1}{l_2} + \omega_{\beta_2}^2}, c_2 = 2\eta_2\omega\beta_2, d_2 = \frac{k_5}{\Omega^2 R^2 l_2^2 m_0},$$

$$e_2 = \frac{k_6}{\Omega^2 R^2 l_2^2 m_0}, f_2 = \frac{\omega^2 y_0}{l_2}. \text{ Among them, } \gamma = \frac{m_0}{mR}, \omega = \frac{\omega_0}{\Omega}, \Delta = \frac{1}{\frac{1}{3}(1 - e)^3 + (l_1 + l_2)^2\gamma},$$

$$I_b = \frac{1}{3}(1 - e)^3 m R^3, \omega_{\beta_1} = \sqrt{\frac{k_1}{\Omega^2 I_b}}, \eta_1 = \frac{c'_1}{2\Omega\omega_{\beta_1} I_b}, \omega_{\beta_2} = \sqrt{\frac{k_4}{\Omega^2 R^2 l_2^2 m_0}}, \eta_2 = \frac{c'_2}{2\Omega\omega_{\beta_2} R^2 l_2^2 m_0}.$$

In order to decouple the inertia and elastic terms in Eq. (11) and Eq. (12), we use coordinate transformations:

$$\begin{pmatrix} \beta_1 \\ \beta_2 \end{pmatrix} = Q \begin{pmatrix} x_1 \\ x_2 \end{pmatrix}, \tag{13}$$

where x_1, x_2 are the principal coordinates of undamped derivation system and $Q = \begin{pmatrix} 1 & 1 \\ q_{21} & q_{22} \end{pmatrix}$.

$$q_{21} = -\frac{\omega_1^2 - \frac{-a_2 b_1 - a_1 b_2 + \omega_1^2 + \omega_2^2 - \sqrt{(a_2 b_1 + a_1 b_2 - \omega_1^2 - \omega_2^2)^2 - 4(1 - a_1 a_2)(-b_1 b_2 + \omega_1^2 \omega_2^2)}}{2(1 - a_1 a_2)}}{a_1 \left(-a_2 b_1 - a_1 b_2 + \omega_1^2 + \omega_2^2 - \sqrt{(a_2 b_1 + a_1 b_2 - \omega_1^2 - \omega_2^2)^2 - 4(1 - a_1 a_2)\sqrt{-b_1 b_2 + \omega_1^2 \omega_2^2}} \right)}$$

$$b_1 - \frac{2(1 - a_1 a_2)}{a_1 \left(-a_2 b_1 - a_1 b_2 + \omega_1^2 + \omega_2^2 - \sqrt{(a_2 b_1 + a_1 b_2 - \omega_1^2 - \omega_2^2)^2 - 4(1 - a_1 a_2)\sqrt{-b_1 b_2 + \omega_1^2 \omega_2^2}} \right)}$$

$$q_{22} = -\frac{\omega_1^2 - \frac{-a_2 b_1 - a_1 b_2 + \omega_1^2 + \omega_2^2 - \sqrt{(a_2 b_1 + a_1 b_2 - \omega_1^2 - \omega_2^2)^2 - 4(1 - a_1 a_2)(-b_1 b_2 + \omega_1^2 \omega_2^2)}}{2(1 - a_1 a_2)}}{a_1 \left(-a_2 b_1 - a_1 b_2 + \omega_1^2 + \omega_2^2 + \sqrt{(a_2 b_1 + a_1 b_2 - \omega_1^2 - \omega_2^2)^2 - 4(1 - a_1 a_2)\sqrt{-b_1 b_2 + \omega_1^2 \omega_2^2}} \right)}$$

$$b_1 - \frac{2(1 - a_1 a_2)}{a_1 \left(-a_2 b_1 - a_1 b_2 + \omega_1^2 + \omega_2^2 + \sqrt{(a_2 b_1 + a_1 b_2 - \omega_1^2 - \omega_2^2)^2 - 4(1 - a_1 a_2)\sqrt{-b_1 b_2 + \omega_1^2 \omega_2^2}} \right)}$$

Then the original equations Eq. (11) and Eq. (12) can be transformed into equivalent principal coordinate equations with inertia and elastic decoupling as:

$$x_1'' + \omega_{n_1}^2 x_1 = \varepsilon(-\gamma_1 x_1' + \gamma_2 x_2' + \mu_1 x_1^2 + \mu_2 x_1 x_2 + \mu_3 x_2^2 + v_1 x_1^3 + v_2 x_1^2 x_2 + v_3 x_1 x_2^2 + v_4 x_2^3) + p_1 \cos(\omega\psi), \tag{14}$$

$$x_2'' + \omega_{n_2}^2 x_2 = \varepsilon(\gamma_3 x_1' - \gamma_4 x_2' + \mu_4 x_1^2 + \mu_5 x_1 x_2 + \mu_6 x_2^2 + v_5 x_1^3 + v_6 x_1^2 x_2 + v_7 x_1 x_2^2 + v_8 x_2^3) + p_2 \cos(\omega\psi), \tag{15}$$

where:

$$\omega_{n_{1,2}}^2 = \frac{1}{2(1 - a_1 a_2)} \left[\pm \sqrt{\omega_1^2 + \omega_2^2 - a_1 b_2 - a_2 b_1} \right]$$

Since the other coefficients of Eq. (14) and Eq. (15) are too complex, using symbols instead of them, and the specific forms are omitted here.

3. Combination resonance analysis

Utilizing multiple scales method, the first-order approximate solution of Eq. (14) and Eq. (15) can be expanded as:

$$x_i(\psi, \varepsilon) = x_{i0}(T_0, T_1) + \varepsilon x_{i1}(T_0, T_1), \quad i = 1, 2, \tag{16}$$

where $T_0 = \psi$ is fast variable, and $T_1 = \varepsilon\psi$ is slow variable. Suppose:

$$\frac{d}{d\psi} = \frac{\partial}{\partial T_0} \frac{dT_0}{d\psi} + \frac{\partial}{\partial T_1} \frac{dT_1}{d\psi} = D_0 + \varepsilon D_1, \tag{17}$$

$$\frac{d}{d\psi} = \frac{\partial}{\partial T_0} \frac{dT_0}{d\psi} + \frac{\partial}{\partial T_1} \frac{dT_1}{d\psi} = D_0 + \varepsilon D_1. \tag{18}$$

Applying the relation of Eq. (17) and Eq. (18), we obtain:

$$\begin{cases} D_0^2 x_{10} + \omega_{n_1}^2 x_{10} = p_1 \cos(\omega\psi), \\ D_0^2 x_{20} + \omega_{n_2}^2 x_{20} = p_2 \cos(\omega\psi), \end{cases} \tag{19}$$

$$\begin{cases} D_0^2 x_{11} + \omega_{n_1}^2 x_{11} = \left(-2D_0 D_1 x_{10} - \gamma_1 D_0 x_{10} + \gamma_2 D_0 x_{20} + \mu_1 x_{10}^2 + \mu_2 x_{10} x_{20} \right. \\ \quad \left. + \mu_3 x_{20}^2 + v_1 x_{10}^3 + v_2 x_{10}^2 x_{20} + v_3 x_{10} x_{20}^2 + v_4 x_{20}^3 \right), \\ D_0^2 x_{21} + \omega_{n_2}^2 x_{21} = \left(-2D_0 D_1 x_{20} + \gamma_3 D_0 x_{10} - \gamma_4 D_0 x_{20} + \mu_4 x_{10}^2 + \mu_5 x_{10} x_{20} \right. \\ \quad \left. + \mu_6 x_{20}^2 + v_5 x_{10}^3 + v_6 x_{10}^2 x_{20} + v_7 x_{10} x_{20}^2 + v_8 x_{20}^3 \right). \end{cases} \tag{20}$$

The solutions of zero-order approximate Equation (19) can be expressed as:

$$x_{10} = A_1(T_1) \exp(i\omega_{n_1} T_0) + B_1 \exp(i\omega T_0) + cc, \tag{21}$$

$$x_{20} = A_2(T_1) \exp(i\omega_{n_2} T_0) + B_2 \exp(i\omega T_0) + cc, \tag{22}$$

where A_i is plural form free vibration amplitude, and B_i is real form forced vibration amplitude, $B_i = \frac{p_i}{2(\omega_{n_i}^2 - \omega^2)}$, $i = 1, 2$. cc represents the conjugate term of all the previous terms.

Substitute zero-order approximate solutions (21) and (22) into first-order Eq. (20). By frequency combination relation $\omega = \omega_{n_1} + \omega_{n_2} + \varepsilon\sigma$ (σ is a tuning parameter), secular terms can be eliminated. We obtain the following equations with respect to A_1, A_2 :

$$-2i\omega_{n_1} A_1' - \gamma_1 i\omega_{n_1} A_1 + 2v_3 A_1 A_2 \bar{A}_2 + 6v_1 A_1 B_1^2 + 3v_1 A_1^2 \bar{A}_1 + 4v_2 A_1 B_1 B_2 + 2v_3 A_1 B_2^2 + (\mu_2 \bar{A}_2 B_1 + 2\mu_3 \bar{A}_2 B_2) \exp(i\sigma T_1) = 0, \tag{23}$$

$$-2i\omega_{n_2} A_2' - \gamma_4 i\omega_{n_2} A_2 + 2v_6 A_1 A_2 \bar{A}_1 + 6v_8 A_2 B_2^2 + 3v_8 A_2^2 \bar{A}_2 + 4v_7 A_2 B_1 B_2 + 2v_6 A_2 B_1^2 + (\mu_5 \bar{A}_1 B_2 + 2\mu_4 \bar{A}_1 B_1) \exp(i\sigma T_1) = 0, \tag{24}$$

where $()' = \frac{d}{dT_1}$ and $\bar{()}$ represents conjugated term. From the process of eliminating secular terms, it can be seen that when using multiple scales method to investigate nonlinear effect on motion characteristics of blade-absorber system, only combination resonance in $\omega \approx \omega_{n_1} + \omega_{n_2}$ case can be considered.

Suppose $A_1(T_1) = (g_{r1} + i g_{i1}) \exp\left(\frac{1}{2} i\sigma T_1\right)$, $A_2(T_1) = (g_{r2} + i g_{i2}) \exp\left(\frac{1}{2} i\sigma T_1\right)$, where g_{r1}, g_{i1}, g_{r2} and g_{i2} are all real number. Substituting A_1 and A_2 into Eq. (23), (24) yields:

$$g_{r1}' = -\frac{\gamma_1}{2} g_{r1} + \left(\frac{\sigma}{2} + \frac{L}{\omega_{n_1}}\right) g_{i1} - \frac{K}{2\omega_{n_1}} g_{i2} + \frac{3v_1}{2\omega_{n_1}} g_{i1} (g_{i1}^2 + g_{r1}^2) + \frac{v_3}{\omega_{n_1}} g_{i1} (g_{r2}^2 + g_{i2}^2), \tag{25}$$

$$g'_{i1} = -\left(\frac{\sigma}{2} + \frac{L}{\omega_{n1}}\right)g_{r1} - \frac{\gamma_1}{2}g_{i1} - \frac{K}{2\omega_{n1}}g_{r2} - \frac{3v_1}{2\omega_{n1}}g_{i1}(g_{i1}^2 + g_{r1}^2) - \frac{v_3}{\omega_{n1}}g_{i1}(g_{r2}^2 + g_{i2}^2), \quad (26)$$

$$g'_{r2} = -\frac{M}{2\omega_{n2}}g_{i1} - \frac{\gamma_4}{2}g_{r2} + \left(\frac{\sigma}{2} + \frac{N}{\omega_{n2}}\right)g_{i2} + \frac{3v_8}{2\omega_{n2}}g_{i2}(g_{r2}^2 + g_{i2}^2) + \frac{v_6}{\omega_{n2}}g_{i2}(g_{r1}^2 + g_{i1}^2), \quad (27)$$

$$g'_{i2} = -\frac{M}{2\omega_{n2}}g_{r1} - \left(\frac{\sigma}{2} + \frac{N}{\omega_{n2}}\right)g_{r2} - \frac{\gamma_4}{2}g_{i2} - \frac{3v_8}{2\omega_{n2}}g_{r2}(g_{r2}^2 + g_{i2}^2) - \frac{v_6}{\omega_{n2}}g_{i2}(g_{r1}^2 + g_{i1}^2), \quad (28)$$

where $K = \mu_2 B_1 + 2\mu_3 B_2$, $L = 2v_2 B_1 B_2 + 3v_1 B_1^2 + v_3 B_2^2$, $N = 2v_7 B_1 B_2 + 3v_8 B_2^2 + v_6 B_1^2$, $M = \mu_5 B_2 + 2\mu_4 B_1$.

The Jacobi matrix of system (25) to (28) on the initial equilibrium solution $(g_{r1}, g_{i1}, g_{r2}, g_{i2}) = (0,0,0,0)$ is:

$$J = \begin{bmatrix} -\frac{\gamma_1}{2} & \frac{\sigma}{2} + \frac{L}{\omega_{n1}} & 0 & -\frac{K}{2\omega_{n1}} \\ -\left(\frac{\sigma}{2} + \frac{L}{\omega_{n1}}\right) & -\frac{\gamma_1}{2} & -\frac{K}{2\omega_{n1}} & 0 \\ 0 & -\frac{M}{2\omega_{n2}} & -\frac{\gamma_4}{2} & \frac{\sigma}{2} + \frac{N}{\omega_{n2}} \\ -\frac{M}{2\omega_{n2}} & 0 & -\left(\frac{\sigma}{2} + \frac{N}{\omega_{n2}}\right) & -\frac{\gamma_4}{2} \end{bmatrix}. \quad (29)$$

The characteristic polynomial of matrix (29) can be written as:

$$f(\lambda) = \lambda^4 + R_1\lambda^3 + R_2\lambda^2 + R_3\lambda + R_4, \quad (30)$$

where:

$$\begin{aligned} R_1 &= \gamma_1 + \gamma_4, \quad R_2 = \frac{\gamma_1^2}{4} + \gamma_1\gamma_4 + \frac{\gamma_4^2}{4} + \frac{\sigma^2}{2} + \frac{L^2}{\omega_{n1}^2} + \frac{L\sigma}{\omega_{n1}} + \frac{N^2}{\omega_{n2}^2} + \frac{N\sigma}{\omega_{n2}} - \frac{KM}{2\omega_{n1}\omega_{n2}}, \\ R_3 &= \frac{1}{4} \left[\gamma_1^2\gamma_4 + \gamma_1\gamma_4^2 + \gamma_1\sigma^2 + \gamma_4\sigma^2 - \frac{KM(\gamma_1 + \gamma_4)}{\omega_{n1}\omega_{n2}} \right] + \frac{L^2\gamma_4}{\omega_{n1}^2} + \frac{L\gamma_4\sigma}{\omega_{n1}} + \frac{N^2\gamma_1}{\omega_{n2}^2} + \frac{N\gamma_1\sigma}{\omega_{n2}}, \\ R_4 &= \frac{1}{16} \left(\gamma_1^2\sigma^2 + \gamma_4^2\sigma^2 + \sigma^4 + \frac{K^2M^2 - 8KMLN + 16L^2N^2}{\omega_{n1}^2\omega_{n2}^2} + \gamma_1^2\gamma_4^2 \right) \\ &+ \frac{1}{4} \left[\frac{L^2(\gamma_4^2 + \sigma^2)}{\omega_{n1}^2} + \frac{L(\gamma_4^2\sigma + \sigma^3)}{\omega_{n1}} + \frac{N^2(\gamma_1^2 + \sigma^2)}{\omega_{n2}^2} + \frac{LN^2\sigma - KMN\sigma}{\omega_{n1}\omega_{n2}^2} + \frac{N\gamma_1^2\sigma + N\sigma^3}{\omega_{n2}} \right. \\ &\left. + \frac{L^2N\sigma - KLM\sigma}{\omega_{n1}^2\omega_{n2}} \right] - \frac{KM(\gamma_1\gamma_4 + \sigma^2)}{8\omega_{n1}\omega_{n2}} + \frac{LN\sigma^2}{\omega_{n1}\omega_{n2}}. \end{aligned}$$

By Hurwitz criterion, when:

$$R_1 > 0, \quad R_1R_2 - R_3 > 0, \quad R_3(R_1R_2 - R_3) - R_1^2R_4 > 0, \quad R_4 > 0. \quad (31)$$

The initial equilibrium solution $(g_{r1}, g_{i1}, g_{r2}, g_{i2}) = (0,0,0,0)$ is stable, otherwise the initial equilibrium solution is unstable, and bifurcation may occur.

4. Stability and bifurcation analysis

4.1. The case of a pair of pure imaginary eigenvalues

If:

$$\frac{R_3}{R_1} \left(\frac{R_3}{R_1} - R_2 \right) + R_4 = 0, \quad \frac{R_3}{R_1} > 0, \quad R_1 > 0, \quad R_4 > 0, \quad (32)$$

the eigenvalues of matrix (29) are $\lambda_{1,2} = \pm \sqrt{\frac{R_3}{R_4}}$, $\lambda_{3,4} = -\sigma_1 \pm i\sigma_2$, ($\sigma_i > 0, i = 1, 2$). Thus the stability of the initial equilibrium is violated and Hopf bifurcation may occur.

In the calculation, the values of dimensionless parameters are taken as follows:

$$e = 0.05, \quad \omega_{\beta_1} = 2, \quad \omega_{\beta_2} = 0.1, \quad \eta_1 = \eta_2 = 0.01, \quad \gamma = 0.15, \quad d_1 = 1, \quad e_1 = 5, \quad (33)$$

$$d_2 = 0.001, \quad e_2 = 0.001, \quad l_1 = 0.01, \quad y_0 = 0.1, \quad l_2 = 0.0154, \quad \sigma = \sigma_0 = 0.1.$$

The above data are partly based on Boeing Vertol 347 helicopter and the reference [13]. The eigenvalues of Jacobi matrix (29) are $\lambda_{1,2} = \pm 0.17688i$ and $\lambda_{3,4} = -0.0007156 \pm 0.03411i$.

Considering parameter σ as a perturbation parameter and using the parameter transformation $\sigma = \sigma_0 + \delta$ as well as the state variable transform:

$$\begin{bmatrix} g_{r1} \\ g_{i1} \\ g_{r2} \\ g_{i2} \end{bmatrix} = \begin{bmatrix} 2.1601 & 0.51986 & -1.74213 & -0.03655 \\ -0.51986 & 2.1601 & -0.03655 & 1.74213 \\ 1.09371 & -0.04591 & -0.38763 & -0.12941 \\ -0.04591 & -1.09371 & 0.12941 & -0.38763 \end{bmatrix} \begin{bmatrix} z_1 \\ z_2 \\ z_3 \\ z_4 \end{bmatrix}. \quad (34)$$

System (25)-(28) can be rewritten as:

$$z_1' = 0.17688z_2 - 0.25993\delta z_1 + 1.08005\delta z_2 + 0.01828\delta z_3 - 0.87107\delta z_4 + f_1, \quad (35)$$

$$z_2' = -0.17688z_1 - 1.08005\delta z_1 - 0.25993\delta z_2 - 0.87107\delta z_3 - 0.01828\delta z_4 + f_2, \quad (36)$$

$$z_3' = -0.0007156z_3 + 0.03411z_4 + 0.02296\delta z_1 + 0.54685\delta z_2 + 0.0647\delta z_3 - 0.19381\delta z_4 + f_3, \quad (37)$$

$$z_4' = -0.03411z_3 - 0.0007156z_4 + 0.54685\delta z_1 - 0.02296\delta z_2 + 0.19381\delta z_3 + 0.0647\delta z_4 + f_4, \quad (38)$$

where f_i ($i = 1, 2, 3, 4$) represent nonlinear terms. For brevity, the specific forms of f_i are omitted here. The Jacobi matrix evaluated on the initial equilibrium solution $(z_1, z_2, z_3, z_4) = (0, 0, 0, 0)$ at the critical point $\delta = 0$ is now in the canonical form:

$$J_{(z_i=0)} = \begin{bmatrix} 0 & 0.17688 & 0 & 0 \\ -0.17688 & 0 & 0 & 0 \\ 0 & 0 & -0.0007156 & 0.03411 \\ 0 & 0 & -0.03411 & -0.0007156 \end{bmatrix}. \quad (39)$$

The local dynamic behaviors of system (35) to (38) are characterized by the critical variables z_1 and z_2 . Using the normal form method in reference [3] and the time scaling transformation

$\tau = \frac{\tau'}{0.17688}$, we can obtain the normal form in a polar coordinate system as follows:

$$\frac{dr}{d\tau'} = a\delta r + br^3, \quad (40)$$

$$\frac{d\theta}{d\tau'} = 1 + c\delta r + dr^3, \tag{41}$$

where $a = -1.46953$, $b = 184.88595$, $c = 6.10612$, $d = -113.15805$. The steady state solutions of (40) are determined by setting $\frac{dr}{d\tau'} = 0$, which yields the initial equilibrium $r_1 = 0$ and Hopf bifurcation solution:

$$r_2^2 = 0.01297\delta. \tag{42}$$

The stability of these two steady state solutions are determined by:

$$\frac{d}{dr} \left(\frac{dr}{d\tau'} \right) = a\delta + 3br^2. \tag{43}$$

Evaluating (43) on the initial equilibrium $r_1 = 0$ yields $\frac{d}{dr} \left(\frac{dr}{d\tau'} \right) = -1.46953\delta$. The initial equilibrium is stable when $\delta > 0$ and unstable when $\delta < 0$. In the same way, evaluating (43) on Hopf bifurcation solution (42) yields $\frac{d}{dr} \left(\frac{dr}{d\tau'} \right) = 5.72438\delta$. So Hopf bifurcation solution (43) is unstable when $\delta > 0$ and no meaning when $\delta < 0$. The bifurcation path is shown in Fig. 2. Fig. 3 displays unsteady Hopf bifurcation solution. From the above situations and Eq. (42), we can conclude that when $\delta > 0$ the stable region of system (25) to (28) is very small, and system response is easy to diverge. Therefore the original blade-absorber system is also extremely sensitive, and this is a very dangerous situation in engineering.

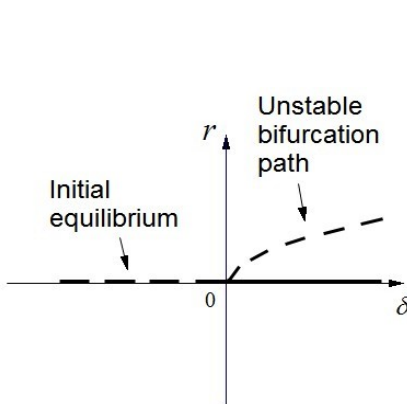


Fig. 2. Bifurcation path

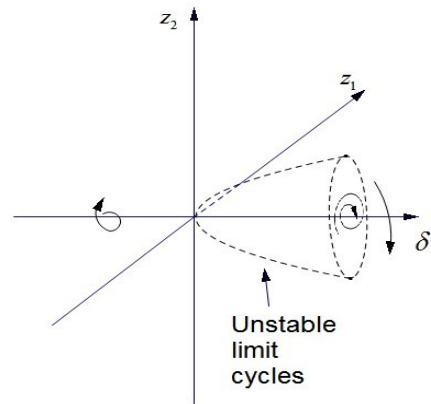


Fig. 3. Unstable Hopf bifurcation solution

Now different values of parameter δ are chosen to confirm the previous analytical results. Fourth-order Runge-Kutta method is adopted to simulate the response of Equations (25)-(28). Since this study focuses on local dynamic behaviors in the vicinity of critical point, the parameter δ should be chosen near the critical point $\delta = 0$.

If the parameter is chosen as $\delta = 0.001$, a numerical solution starting from the initial point $(g_{r1}, g_{i1}, g_{r2}, g_{i2}) = (0.01, 0.01, 0.01, 0.01)$ converges to the initial equilibrium solution, i.e. initial equilibrium solution is stable. It is indicative that system (25)-(28) disturbed by a small perturbation can still return its original state, which is shown in Fig. 4. Choosing the parameter as $\delta = -0.001$ and starting from $(g_{r1}, g_{i1}, g_{r2}, g_{i2}) = (0.1, 0.01, 0.01, 0)$, system response is divergence. It is indicative that system will produce large amplitude vibration, thereby causing damage to the whole structure. The numerical results are in good agreement with the theoretical analysis.

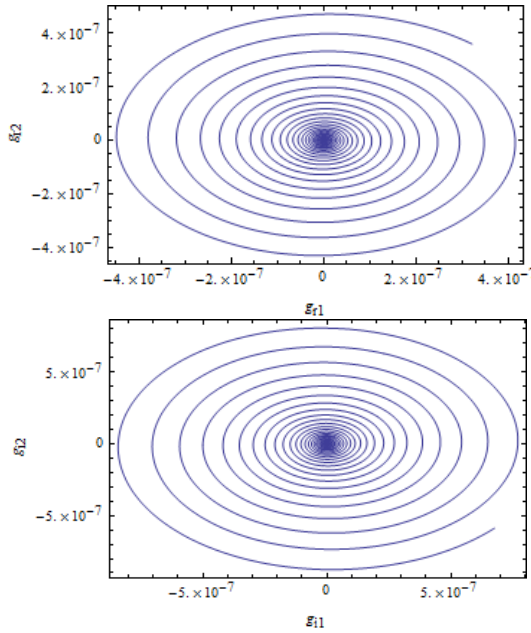


Fig. 4. Trajectory projections converge to the initial equilibrium solution when $\delta = 0.001$

4.2. The case of double zero eigenvalues

Taking parameters as follows:

$$\begin{aligned}
 e = 0.05, \quad \omega_{\beta_1} = 1.75518, \quad \omega_{\beta_2} = 0.1, \quad \eta_1 = \eta_2 = 0.01, \quad \gamma = 0.15, \quad d_1 = 1, \\
 e_1 = 5, \quad d_2 = 0.001, \quad e_2 = 0.001, \quad l_1 = 0.01, \quad l_2 = 0.02, \quad \omega_{\beta_1} = 2, \quad \sigma = \sigma_0 = 0.1, \\
 y_0 = 0.597817.
 \end{aligned}
 \tag{44}$$

Jacobi matrix (29) has the eigenvalues $\lambda_{1,2} = 0$, $\lambda_{3,4} = -0.16099 \pm 1.36954i$. We consider parameters ω_{β_1} and y_0 perturbation parameters and use the parameter transformation $\omega_{\beta_1} = 1.75518 + \delta_1$, $y_0 = 0.597817 + \delta_2$. Then characteristic polynomial of the Jacobi matrix (29) becomes:

$$\tilde{f}(\lambda) = \lambda^4 + \tilde{R}_1 \lambda^3 + \tilde{R}_2 \lambda^2 + \tilde{R}_3 \lambda + \tilde{R}_4,
 \tag{45}$$

where the specific forms of \tilde{R}_i ($i = 1, 2, 3, 4$) are too complex then omitted.

By Hurwitz criterion, the stability conditions for the initial equilibrium solution $(g_{r1}, g_{i1}, g_{r2}, g_{i2}) = (0, 0, 0, 0)$ are:

$$\Delta_1 = \tilde{R}_1 > 0, \quad \Delta_2 = \tilde{R}_1 \tilde{R}_2 - \tilde{R}_3 > 0, \quad \Delta_3 = \tilde{R}_1 \tilde{R}_2 - \tilde{R}_3 > 0, \quad \Delta_4 = \tilde{R}_4 > 0.
 \tag{46}$$

From the four inequalities above, we get the following four transition curves:

$$L_1: \tilde{R}_1 = 0, \quad L_2: \tilde{R}_1 \tilde{R}_2 - \tilde{R}_3 = 0, \quad L_3: \tilde{R}_1 \tilde{R}_2 - \tilde{R}_3 = 0, \quad L_4: \tilde{R}_4 = 0.
 \tag{47}$$

Since system local property near $(\delta_1, \delta_2) = (0, 0)$ is only considered, $L_4 > 0$ always holds in this region. Therefore when $L_i > 0$ ($i = 1, 2, 3$), initial equilibrium solution is stable, otherwise it is unstable. The transition curves in the vicinity of $(\delta_1, \delta_2) = (0, 0)$ and stable region (shaded part) for initial equilibrium solution (E.S.) are shown in Fig. 5.

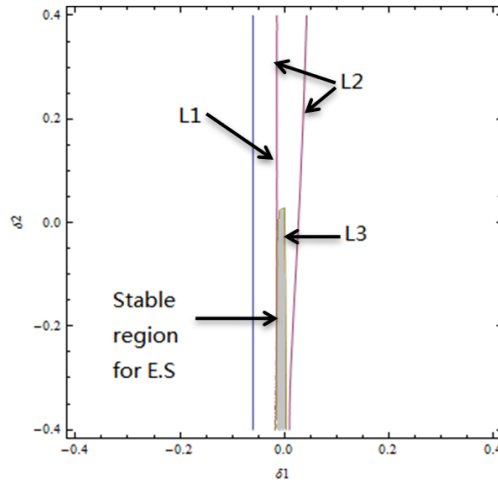


Fig. 5. Transition curves and stable region in the case of double zero eigenvalue

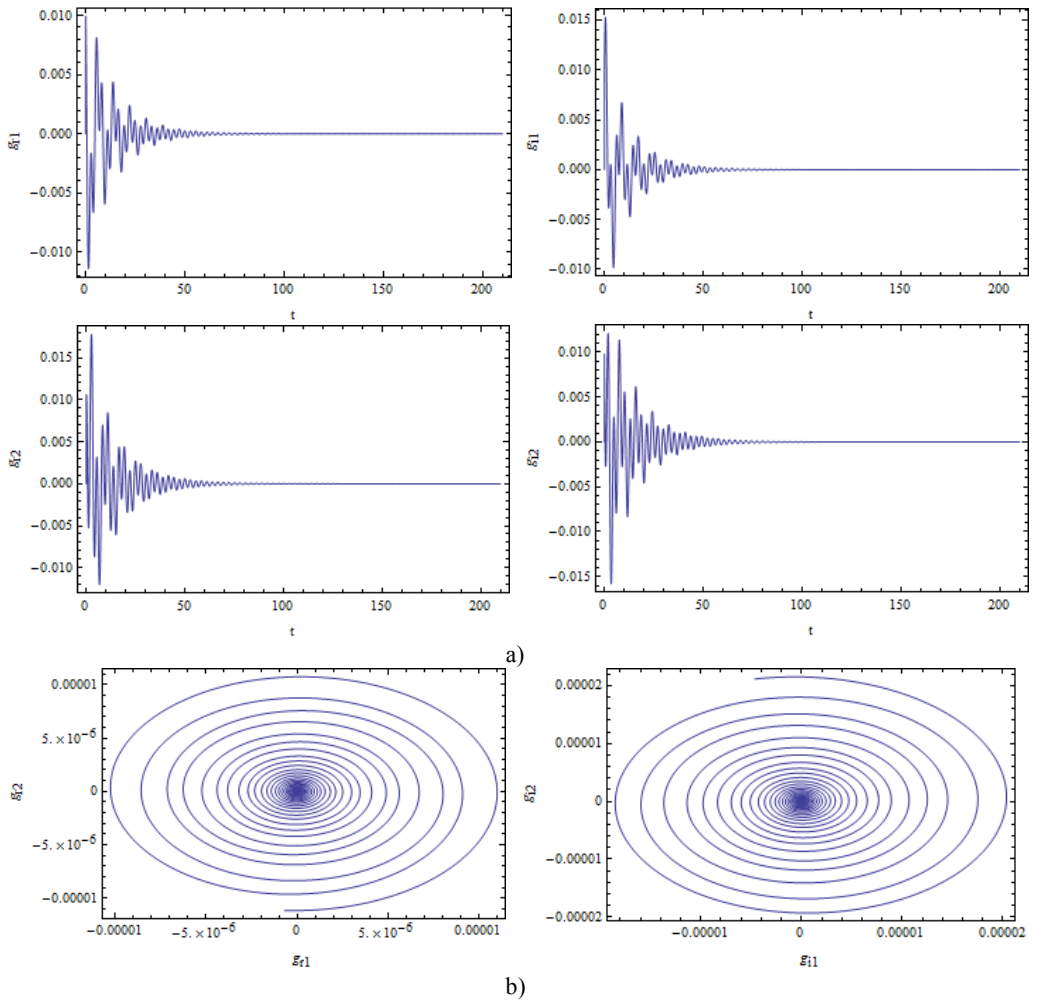


Fig. 6. a) $g_{r1}, g_{i1}, g_{r2}, g_{i2}$ response process and b) phase diagrams of convergence to the origin

Now we will confirm the previous analysis by fourth-order Runge-Kutta method. Choosing parameter values of δ_1 and δ_2 from the stable region for E.S., such as $(\delta_1, \delta_2) = (-0.001, 0.01)$, a numerical solution starting from an initial point $(g_{r1}, g_{i1}, g_{r2}, g_{i2}) = (0.01, 0.01, 0.01, 0.01)$ converges to the origin, implying that the E.S. is stable. $g_{r1}, g_{i1}, g_{r2}, g_{i2}$ response process as well as phase diagram projection on the g_{r1} - g_{r2} and g_{i1} - g_{i2} sub-spaces are shown in Fig. 6.

5. Conclusions

In this work, the dynamic behaviors of a helicopter blade-absorber model have been studied in detail. The research shows that helicopter blade-absorber vibration system has relatively rich in dynamic behaviors, and its dynamic analysis is of great necessity. When the stable conditions for the initial equilibrium solution of the bifurcation response equations are not satisfied, two kinds of critical points (characterized by a pair of purely imaginary eigenvalues and double zero eigenvalues) have been considered. Bifurcation path, transition curves and stable region have been obtained. All analytical predictions are agree with numerical results calculated by Runge-Kutta method. Note that in the blade-absorber system vibration process, the appearance of unstable Hopf solution is extremely dangerous, we should apply a bifurcation control or avoid taking system parameter in the vicinity of bifurcation point. Therefore, in order to achieve the purpose of absorbing vibration, ensure system safety, when designing system parameter, we must fully consider external excitation frequency, avoid the possible resonance region, and retain a certain safety margin.

Acknowledgements

This paper is supported by Specialized Research Fund for the Doctoral Program of Higher Education of China (No. 20113218110002) and a project funded by the Priority Academic Program Development of Jiangsu Higher Education Institutions of China.

References

- [1] **Yu P.** Analysis on double Hopf bifurcation using computer algebra with the aid of multiple scales. *Nonlinear Dyn.*, Vol. 27, 2002, p. 19-53.
- [2] **Bi Q., Yu P.** Symbolic computation of normal forms for semi-simple cases. *Journal of Comput. and Appl. Math.*, Vol. 102, 1999, p. 195-220.
- [3] **Yu P.** Computation of norm forms via a perturbation technique. *Journal of Sound and Vibration*, Vol. 211, 1998, p. 19-38.
- [4] **Yu P.** Symbolic computation of normal forms for resonant double Hopf bifurcations using a perturbation technique. *Journal of Sound and Vibration*, Vol. 247, 2001, p. 615-632.
- [5] **Yu P., Yuan Y.** The simplest normal form for the singularity of a pure imaginary pair and a zero eigenvalue. *Dynamics of Continuous, Discrete and Impulsive Systems Series B, Application & Algorithms*, Vol. 8, Issue 2, 2001, p. 219-249.
- [6] **Yu P., Zhu S.** Computation of the normal forms for general M-DOF systems using multiple time scales. Part I: Autonomous systems. *Commun Nonlinear Sci Numer Simulat*, Vol. 10, Issue 8, 2005, p. 869-905.
- [7] **Zhu S., Yu P.** Computation of the normal forms for general M-DOF systems using multiple time scales. Part II: Non-autonomous systems. *Commun Nonlinear Sci Numer Simulat*, Vol. 11, Issue 1, 2006, p. 45-81.
- [8] **Han M., Yang J., Yu P.** Hopf bifurcations for near-Hamiltonian systems. *J. Bifurcation & Chaos*, Vol. 19, Issue 12, 2009, p. 4117-4130.
- [9] **Zhang X. H.** Local bifurcations of nonlinear viscoelastic panel in supersonic flow. *Commun Nonlinear Sci Numer Simulat*, Vol. 18, 2013, p. 1931-1938.
- [10] **Zhang X. H., Chen F. Q., Zhang H. L.** Stability and local bifurcation of functionally graded material plate under transversal and in-plane excitations. *Applied Mathematical Modelling*, Vol. 37, Issue 10-11, 2013, p. 6639-6651.

- [11] **Zhou L. Q., Chen F. Q.** Stability and bifurcation analysis for a model of a nonlinear coupled pitch-roll ship. *Mathematics and Computers in Simulation*, Vol. 79, 2008, p. 149-166.
- [12] **Wang X., Chen F. Q., Zhou L. Q.** Stabilities and bifurcation for a flexible beam under a large linear motion with a combination parametric resonance. *Nonlinear Dynamics*, Vol. 56, 2009, p. 101-119.
- [13] **Sang J. X.** Study on dynamic stability and bifurcation of helicopters. Nanjing University of Aeronautics and Astronautics, 1995, (in Chinese).
- [14] **Bramwell A. R. S., Done G., Balmford D.** *Bramwell's helicopter dynamics*. Second edition, Butterworth-Heinenmann, 2001.
- [15] **Lee C. T., Shaw S. W.** The non-linear dynamic response of paired centrifugal pendulum vibration absorbers. *Journal of Sound and Vibration*, Vol. 203, Issue 5, 1997, p. 731-743.
- [16] **Chao C. P., Lee C. T., Shaw S. W.** Non-union dynamics of multiple centrifugal pendulum vibration absorbers. *Journal of Sound and Vibration*, Vol. 204, Issue 6, 1997, p. 769-794.
- [17] **Nester T. M.** Experimental investigation of circular centrifugal pendulum vibration absorbers. Michigan State University, Master's Thesis, 2002.
- [18] **Miao W., Mouzakis T.** Bifilar analysis study. NASA Contractor Report, NASA CR-159227, Vol. 1, 1980.
- [19] **Cassarino S. J., Mouzakis T.** Bifilar analysis user's manual. NASA Contractor Report, NASA CR-159228, Vol. 2, 1980.8.
- [20] **Taylor R. B., Teare P. A.** Helicopter vibration reduction with pendulum absorbers. *Journal of AHS*, Vol. 20, Issue 3, 1975, p. 9-17.
- [21] **Nagasaka I., Ishida Y., Koyama Y.** Vibration suppression of a helicopter blades by pendulum absorbers. *Transactions of the Japan Society of Mechanical Engineers*, Vol. 73, 2007, p. 129-137.
- [22] **Nagasaka I., Ishida Y., Koyama T.** Vibration suppression of a helicopter fuselage by pendulum absorbers: rigid-body blades with aerodynamic excitation force. *Journal of system design and dynamics*, Vol. 2, 2008, p. 1230-1238.